Sensorless Control of AC Drives at Very Low and Zero Speed

Fernando Briz
University of Oviedo. Dept. of Elect., Computer & System Engineering, Gijón, 33204, Spain, fernando@isa.uniovi.es

Abstract: ***The elimination of rotor position/speed sensors in AC drives has been the focus of intensive research for more than two decades, among the expected benefits are cost and size reduction and increased robustness. The methods developed to achieve this goal are commonly referred to as sensorless control.***

Sensorless control techniques for AC machines that rely on the fundamental excitation have been shown to be capable of providing high performance in the medium and high-speed range. However, the performance of these methods decrease as speed decreases, very low-speed control and position control not being feasible. To overcome this limitation, sensorless control methods based on tracking the position of rotor asymmetries have been proposed. These techniques measure the response of the machine when a high-frequency excitation is applied via the inverter. One of their most appealing properties that there is no restriction working at very low or zero speeds, therefore enabling position control.

This paper reviews high frequency signal injection methods for the rotor position/speed sensorless control of AC machines. Principles of operation, implementation and limits will be covered.

I.- Introduction

The elimination of rotor position/velocity sensors (and cabling) in AC drives has been focus of intensive research for more than two decades [1-45]. The methods developed to achieve this goal are commonly referred to as *sensorless control* in the literature.

Sensorless control techniques for AC drives that rely on the fundamental excitation are already capable of providing adequate performance in the medium to high-speed range [1-4]. However, as the speed decreases, the performance of these methods decrease, and eventually fail in the very low-speed range and/or for position control [4]. To overcome this limitation, sensorless control methods based on tracking the position of saliencies (asymmetries) present in the rotor of electric machines have been proposed [3-44]. Such methods have the capability of providing accurate, high-bandwidth, position and speed estimates in the low-speed range, including zero speed. These techniques measure the response of the machine when high-frequency excitation is applied via the inverter, the major differences among the methods are: 1) the type of high frequency excitation, 2) the type and number of signals measured and 3) the signal processing used to estimate the rotor position [7].

This paper discusses high frequency signal injection methods for the rotor position/speed sensorless control of AC machines, as well as their perspectives. The proposed concepts and methods discussed in this paper are applicable, with little or no differences, to surface and interior permanent magnet synchronous machines (SPMSM and IPMSM), synchronous reluctance machines (SynRM), and induction machines (IM).

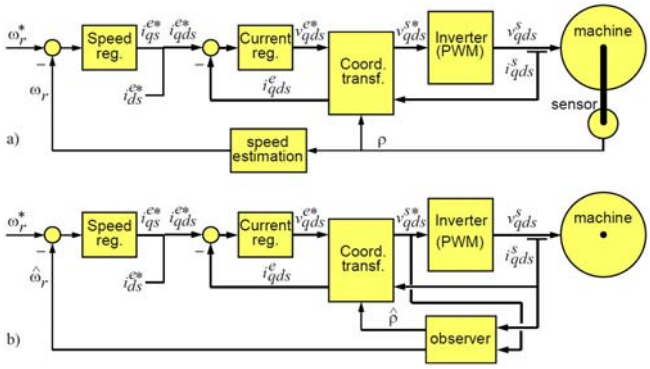

Fig. 1.- Schematic representation of a) sensored and b) sensorless control of an AC machine

II.- Model-base methods: principles and limits

Fig. 1a shows the block diagram of a vector controlled AC drive. The measured rotor position/speed is needed for two purposes: torque/flux control and motion (speed/position) control. Cascaded control, consisting of an inner, high bandwidth current regulator and outer loops for motion control, is often used. For the sensorless implementation, (Fig. 1b), the position/speed sensor (typically an incremental encoder) is removed, some kind of observer derived from the model of the machine is used to estimate the rotor position and speed. The inputs to this model are the electrical terminal quantities, i.e. the stator voltages and currents. While the stator current is normally measured and is therefore available, the stator voltage is practically never measured, the voltage command to the inverter being used instead (see Fig. 1b).

The rotor speed/position can be estimated from the voltage induced in the stator windings due to the rotation of a magnetic field. Eq. (1) shows the stator voltage equation of a SPMSM, the last term in the right side accounting for the back emf. The complex vector of a generic three-phase variable f (current, voltage and flux in the discussion following) is defined as (2).

$$v^s_{qds} = (R + pL)\, i^s_{qds} + j\,\omega_r\,\psi_{pm}\, e^{j\theta_r} \tag{1}$$

$$f^s_{qds} = \frac{2}{3}\,(f_u + f_v\, e^{j2\pi/3} + f_w\, e^{j4\pi/3}) \tag{2}$$

Fig. 2 shows the corresponding phasor diagram. It is observed from (1) and Fig. 2 that the magnitude of the back-emf is proportional to the rotor speed, with its phase angle being function of the rotor position. The rotor speed and position can be readily obtained from (2) using (3), where "^" indicate estimated variables and machine parameters.

$$j\,\hat{\omega}_r\,\hat{\psi}_{pm}\, e^{j\hat{\theta}_r} = v^{s*}_{qds} - (\hat{R} + p\hat{L})\, i^s_{qds} \tag{3}$$

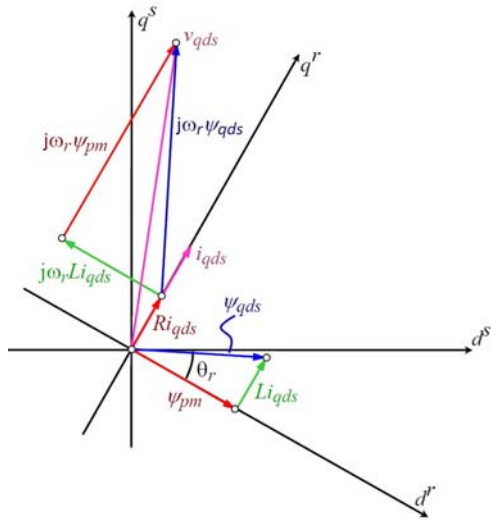

Fig. 2.- The back-emf and the stator flux

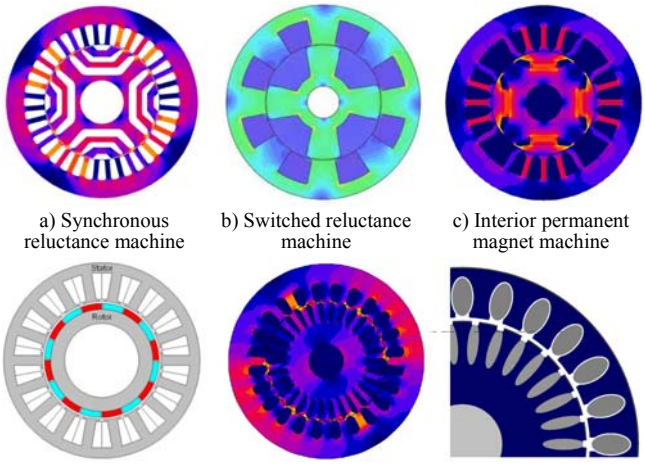

a) Synchronous reluctance machine | b) Switched reluctance machine | c) Interior permanent magnet machine

d) Surface permanent magnet machine | e) Induction machine | f) induction machine with open rotor slots

Fig. 3.- Different machine designs

Unfortunately, the use of (3) presents significant problems. First, the magnitude of the back-emf is proportional to the rotor speed. This means that the back-emf will be reduced at very low speeds, raising signal-to-noise ratio concerns. Furthermore, no back-emf exists at zero speed, meaning that the method cannot be used at zero speed or for position control. In addition, mismatch of the machine parameters used in the model and errors among the actual output voltage and the commanded voltage used in (3), e.g. due to the non-ideal behavior of the inverter, further reduce the accuracy of the method, especially at low speeds.

To overcome the dependency of the back-emf with speed, the stator flux instead of the back-emf can be used. Rearranging the stator voltage equation to include the stator flux, (4)-(5) are obtained.

$$v^s_{qds} = R\, i^s_{qds} + p\, \psi^s_{qds} \tag{4}$$

$$\psi^s_{qds} = L\, i^s_{qds} + \psi_{pm}\, e^{j\theta_r} \tag{5}$$

It is seen from (5) that the stator flux also contains the rotor position information, with the special feature, compared to (3), that its magnitude does not depend on the rotor speed, what would make it adequate for rotor position estimation at very low and zero speed. Unfortunately, the use of the stator flux also has drawbacks. It is observed from (4) that obtaining the stator flux from the stator voltage implies the use of a pure integration. Such open loop integration is not viable in practice. Errors in the voltage command with respect to the actual voltage being injected by the inverter (due e.g. to the dead time in the inverter and voltage drops in the power devices) as well as parameter mismatch, will result in a drift in the estimated stator flux, which becomes more significant as the rotor speed decreases, eventually making the method unviable at very low and zero speed [3, 4].

To overcome the imitations which are intrinsic to (1),(4)-(5), different improvements have been proposed. These go in two directions: 1) incorporation identification/compensation strategies to reduce the errors in the parameters (especially the stator resistance) and variables (e.g. commanded stator voltage), used in the models and 2) design of closed-loop strategies (observers, MRAS, EKF, …) to improve the dynamics, accuracy and operating range of the estimation [4, 5, 7]. While these strategies can provide incremental improvements of the performance of model based methods, still they will unable to operate at zero speed, and consequently to be used position control.

Saliency tracking based sensorless methods were conceived to overcome the limitations of model based methods at low and zero speed, as well as overcome their sensitivity to machine parameters and operating point. Saliency tracking based sensorless methods inject some form of high frequency signal via inverter, which interacts with the rotor asymmetries, to produce some measurable effect in the terminal electrical variables (stator currents/voltages). The use of these methods involves therefore the three key concepts underlined in the previous statement. Rotor asymmetries are discussed in this Section III, high frequency signal injection and measurable effects being discussed in Sections IV to VII.

III.- High frequency modeling of AC machines

Saliency based sensorless methods require that the rotor has some type of electromagnetic asymmetry, which couples with the stator windings to produce measureable effects in the stator electrical variables (currents/voltages). Such asymmetries are intrinsic to certain machine designs, e.g. synchronous reluctance machines (SynRM, Fig. 3a), switched reluctance machines (SRM, Fig. 3b) and interior permanent magnet synchronous machines (IPMSM, Fig. 3c). These designs are said to be *salient*, the common characteristic being that they produce reluctance torque. On the contrary, certain machines designs are non-salient, i.e. the do not produce reluctance torque. Examples of this are surface permanent magnet synchronous machines (SPMSM, Fig. 3d) and induction machines (IM, Fig. 3e and 3f). SynRM, SRM

and IPMSM would be therefore natural candidates for their use with these methods, while SPMSM and IM would not be adequate. However, this is not always true in practice. Secondary effects can make the implementation of the methods a challenging task for machines which would be adequate in principle; on the contrary, they also open nice opportunities for the case of machines being non salient. This issue will be discussed in more detail throughout the paper.

The model of the IPMSM will be used to illustrate the high frequency behavior of salient machines, the extension of this model to SynRM and SPMSM being straightforward. The case of the IM will be discussed later. The fundamental model of the IPMSM in the rotor synchronous reference frame is given by (6), with the d-axis being aligned with the rotor magnet and ψ_{pm} being the magnet flux linkage [27, 28].

$$\begin{bmatrix} v_{qs}^r \\ v_{ds}^r \end{bmatrix} = \begin{bmatrix} R+pL_d & -\omega_r L_q \\ \omega_r L_d & R+pL_q \end{bmatrix} \begin{bmatrix} i_{qs}^r \\ i_{ds}^r \end{bmatrix} + \omega_r \psi_{pm} \begin{bmatrix} 0 \\ 1 \end{bmatrix} \qquad (6)$$

If a high frequency voltage is applied to the stator terminals, several simplifications can be introduced in (6). First, the voltage drops in the resistive terms can be neglected compared to the voltage drops in the inductive terms. Second, due to the high frequency, the *di*/*dt* term in (6) will dominate over the $\omega_r L$ terms. Finally, no high frequency component exists in the back-emf (last term in the right side of (6)). It is concluded that if a high frequency excitation is applied into the stator voltage, the resulting machine model is simplified to (7), which becomes (8) when transformed to the stationary reference frame, with ΣL and ΔL being the average and differential inductances respectively. It is clear from (8) that if a high frequency voltage excitation is applied, the relationship between the stator voltage and current is modulated by the rotor position [27, 28].

$$\begin{bmatrix} v_{qs}^r \\ v_{ds}^r \end{bmatrix} = \begin{bmatrix} L_d & 0 \\ 0 & L_q \end{bmatrix} p \begin{bmatrix} i_{qs}^r \\ i_{ds}^r \end{bmatrix} \qquad (7)$$

$$\begin{bmatrix} v_{qs}^s \\ v_{ds}^s \end{bmatrix} = p \begin{bmatrix} \Sigma L + \Delta L \cos(2\theta_r) & -\Delta L \sin(2\theta_r) \\ \Delta L \sin(2\theta_r) & \Sigma L + \Delta L \cos(2\theta_r) \end{bmatrix} \begin{bmatrix} i_{qs}^s \\ i_{ds}^s \end{bmatrix} \qquad (8)$$

$$\Sigma L = \frac{L_q + L_d}{2} \quad ; \quad \Delta L = \frac{L_q - L_d}{2}$$

The model in (8) is directly applicable to the case of SynRM, as the only difference of this design compared to IPMSM is that there is no permanent magnet exists in the rotor, and it is observed from (7) and (8) that this does not have any influence on the high frequency model.

For the case of SPMSM (Fig. 3d), $L_d \approx L_q$ and therefore $\Delta L \approx 0$, meaning that no rotor position information exists in the currents, as can be deduced from (8). However, saturation due to the magnet field has been reported to produce an asymmetry which can be used for sensorless control purposes [7].

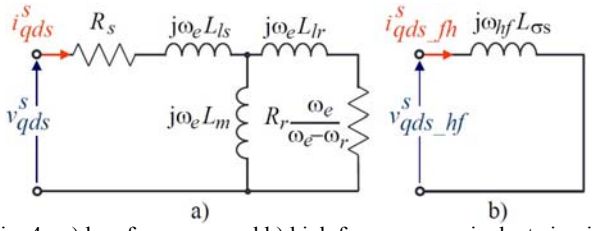

Fig. 4.- a) low frequency and b) high frequency equivalent circuits for an IM

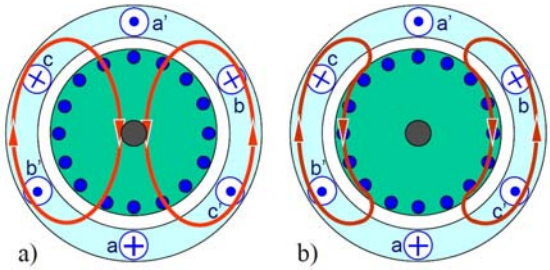

Fig. 5.- a) Low frequency and b) high frequency fluxes for an IM

For the case of IM, the high frequency behavior can be analyzed from the equivalent circuit shown in Fig. 4a. If a high frequency voltage is applied ($\omega_e = \omega_{hf} >> \omega_r$), the equivalent circuit can be simplified to the one shown in Fig. 4b, in which the response is dominated by the stator transient inductance. The different behavior of the circuits in Fig. 4a and 4b is graphically illustrated in Fig. 5. For the case of low frequency excitation ($\omega_e \approx \omega_r$), the flux goes deep into the rotor, linking the rotor bar, eventually inducing currents in the rotor to produce torque. Contrary to this, the high frequency flux (Fig. 5b), does not link the rotor bar, but remains on the rotor surface, meaning that it will *see* asymmetries present on the rotor surface.

IM are not typically designed to have a saliency, meaning that the electromagnetic circuit seen from the stator terminals is usually assumed to be symmetric. However, saliencies exist in standard induction machine designs due to non-linear magnetics (saturation), and due to the effects of rotor and stator slotting [3, 5, 13-16, 22-24, 34, 35, 37, 40]. The presence of stator and rotor slotting in standard induction machine designs inherently creates saliencies that offer the potential for use in sensorless control. Semi-open or open rotor slots are needed, since the rotor slot bridges in closed rotor slot machines offer a low-reluctance path for the high frequency flux, making the rotor slots *invisible* to the high frequency excitation signals [15]. The relationship between the pole number, *p*, number of stator, *S*, and rotor slots, *R*, has to meet the criteria shown in (9) in order for the slotting saliency to couple with the stator windings [13].

$$n \cdot p = |R - S| \quad n = 1,2,4,5,\ldots \qquad (9)$$

If the condition expressed in (9), then (8) can be used to model the high frequency behavior or the IM, by just replacing the term $2\theta_r$ in the 2x2 matrix by $(2R/p)\theta_r$ [13].

If is finally noted that several methods for deliberately creating rotor-position-dependent saliencies in IM have been

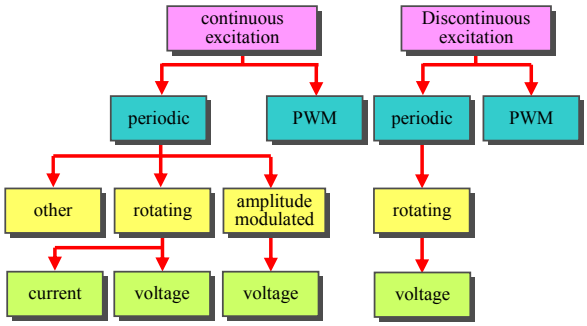

Fig. 6.- Forms of high frequency signal injection that have been proposed

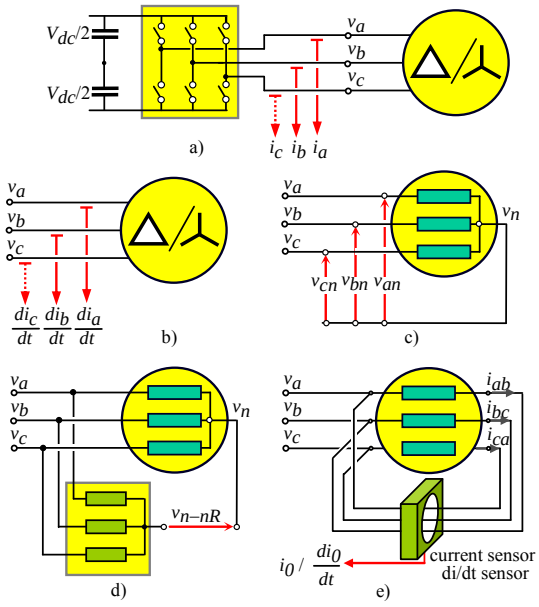

Fig. 7.- Signal measurement: a) phase currents using two/three sensors, b) phase currents derivative using two/three sensors, c) and d) zero sequence voltage using three voltage sensors/a single sensor and an auxiliary resistor network (wye-connected machine), e) zero sequence current/zero sequence current derivative (delta-connected machine)

proposed, [5, 37]. These modifications complicate at a certain level the design and/or manufacturing process of the machine, but might be viable for high volume production.

IV.- High frequency signal injection and signal measurements

As already mentioned, saliency tracking based sensorless methods inject some form of high frequency signal excitation via inverter, and measure the machine response, from which the rotor position is estimated by means of digital signal processing. Since most of electric drives use a voltage source inverter (VSI), the high frequency signal being injected is typically a voltage, the rotor position being estimated from the resulting high frequency stator current. The alternatives for the high frequency signal injection and the signal measurement are discussed following.

High frequency signal injection.-Different forms of high frequency excitations have been proposed, they are shown schematically in Fig. 6 (details can be found in [7]). The proposed methods can be organized using several criteria:

Continuous vs. discontinuous injection: If the high frequency signal used to estimate the rotor position is always present along with the fundamental excitation, it is referred as continuous excitation [5,7-36]. Discontinuous excitation methods inject the high frequency signal periodically, either because they require discontinuing the regular operation of the inverter [6], or to reduce its adverse effects on the normal operation of the machine [37]. However, such methods may require the use of a supplementary observer to estimate the rotor position when the high frequency signal is not injected.

Periodic vs. PWM injection: Tow major concepts have been proposed for the injection of the high frequency signal: 1) use of a periodic high frequency carrier signal (usually in the range of several hundred Hz up to a few kHz) super-imposed on the fundamental excitation, [5,7-31], and 2) use of the fast transients due to the PWM switching, the response to particular states of the inverter is measured in this case [6, 33-36].

Signal measurement.- The number and type of signals that can be measured and processed to obtain the rotor position varies from method-to-method; with more than one option existing for each form of high frequency excitation. Fig. 7 shows the different configuration of the sensors that have been proposed. Most of industrial drives include phase current sensors and often a DC bus voltage sensor. Sensorless methods that rely on only these signals could be considered *no cost* from a hardware perspective (Fig. 7a). Opposite to this are the methods that require additional signals and associated *hardware cost*, e.g., sensors, cabling, A/D channels, signal conditioning circuits, etc (Fig. 7b-7e). In the end, these methods replace a position/speed sensor by a different type of sensor. Methods using zero sequence components have been proposed (Fig. 7c, 7d and 7e), they have the additional drawback of requiring access to the terminal box of the machine, which isn't typically available in industrial drives. It is noted, however, that using sensors which are specific for sensorless control has the benefit of selecting and scaling them for the specific task of measuring the high frequency signals. Detailed discussion of this issue can be found in [7, 16].

Due to room restriction, only two forms of high frequency excitation are discussed in this paper: a rotating high frequency voltage (Section IV) and the PWM commutations (Section V). Discussion of other options can be found in [7, 16].

V.- Rotating high frequency voltage: the negative sequence current

One of the most widely studied forms of high frequency excitation is the injection of a periodic, rotating high frequency signal voltage [15-24]. When a high frequency voltage of the form (10) is applied to the machine, it interacts with the saliencies in the rotor, the resulting high frequency current (11) is obtained by solving (8) for (10) [5].

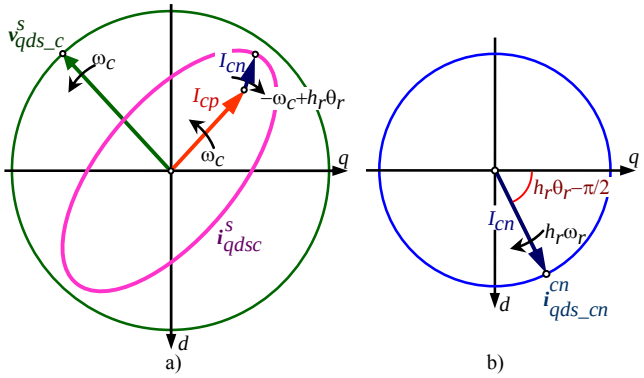

Fig. 8.- a) Complex vector representation of the carrier voltage and resulting carrier current, shown in the stationary reference frame, b) the negative sequence carrier signal current (zoomed), shown in the negative sequence carrier signal reference frame

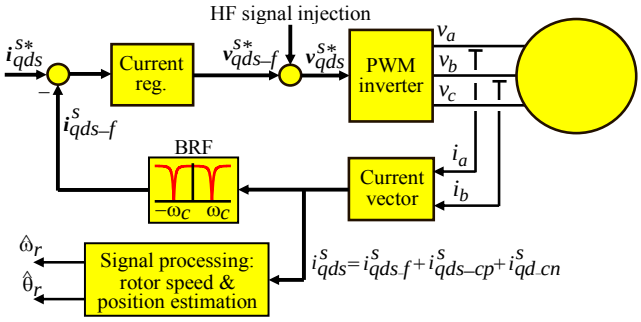

Fig. 9.- Schematic representation of the signal processing of the negative sequence carrier signal current. BRF stands for *band rejection filter* (notch filter)

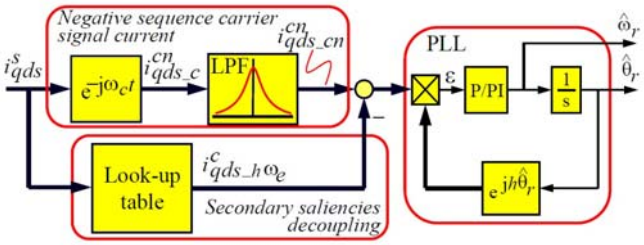

Fig. 10.- Schematic representation of the signal processing of the negative sequence carrier, including the *secondary saliency decoupling* block and the PLL used to estimate the rotor speed and position

$$v^s_{qds\_c} = v^s_{ds\_c} + j\, v^s_{qs\_c} = V_c\, e^{j\omega_c t} \qquad (10)$$

$$i^s_{qds\_c} = -j\, I_{cp}\, e^{j\omega_c t} - j\, I_{cn} e^{j(-\omega_c t + h_r\theta_r)} \qquad (11)$$

$$I_{cp} = \frac{V_c}{\omega_c}\frac{\Sigma L_{\sigma s}}{\Sigma L_{\sigma s}^2 - \Delta L_{\sigma s}^2} \text{ and } I_{cn} = \frac{V_c}{\omega_c}\frac{\Delta L_{\sigma s}}{\Sigma L_{\sigma s}^2 - \Delta L_{\sigma s}^2}$$

The carrier signal current (11), consists of a *positive* and a *negative sequence component*, the second of which contains the rotor position information modulated in its phase. Fig. 8a schematically shows the injected high frequency voltage and the resulting high frequency current. It is noted that (11) only includes the current that results from the carrier signal voltage. In normal operation, the measured stator current will also include the fundamental current used for torque production.

Separation of the different components present in the overall stator current is needed for two purposes. First, the fundamental current is needed for current regulation (and eventually torque control) purposes. Band rejection filters (BRF) can be used to eliminate both the positive and negative components of the high frequency current from the overall current (see Fig. 9), preventing the reaction of the fundamental against the negative sequence carrier signal current containing the desired information.

To isolate the negative sequence carrier signal current, a coordinate transformation to a negative carrier signal reference frame followed by a low-pass filter (LFP) can be used (12) (Fig. 10), the rotor position information being contained in the phase angle of (12), (Fig. 8b).

$$i^{cn}_{qds\_cn} = LPF\left(i^s_{qds\_c}\, e^{j\omega_c t}\right) = -j\, I_{cn} e^{jh_r\theta_r} \qquad (12)$$

Different methods have been proposed to obtain this angle. The use of a tan^{-1} function is very likely the most intuitive solution. However, this option has inconveniences. First, it is computationally expensive. Second, this method only provides $\hat{\theta}_r$. If $\hat{\omega}_r$ is also needed, discrete differentiation of $\hat{\theta}_r$ can be required, which is problematic in practice due to the noise present in the signals. A complex vector PLL can be used instead. A vector cross-product (see Fig. 10) is used to generate an error signal (13) that drives a controller from which the rotor position $\hat{\theta}_r$ is obtained [5, 22, 27].

$$\varepsilon = I_{cn}\, sin(h\,(\theta_r - \hat{\theta}_r)) \approx I_{cn}\,(h\,(\theta_r - \hat{\theta}_r)) \qquad (13)$$

Another important characteristic of the system in Fig. 10 is that the rotor speed $\hat{\omega}_r$, is obtained as an internal variable, eliminating the need of digital differentiation of the estimated rotor position. Other methods available to obtain the rotor position/speed based on the use of tracking observer can be found in [22, 27].

It is finally noted that Fig. 10 includes an additional block labeled as Secondary saliencies decoupling, the purpose of this block is described in Section VII.

VI.- PWM based methods

The response to step-like voltage variations produced by the switching of the inverter have also been shown to be useful for saliency position estimation. Two types of signals have been proposed for their use in wye-connected machines: the *derivative of the current* (*di*/*dt*) [35, 36] and the *zero sequence voltage* induced in the stator windings [32, 33]. Only the second is presented here due to room restrictions.

In the technique proposed in [35, 36], the instantaneous line-to-neutral voltages (see Fig. 7c) are measured. The zero sequence voltage is given by (14), by substituting v_{an}, v_{bn} and v_{bn} by the corresponding voltage levels applied by the inverter.

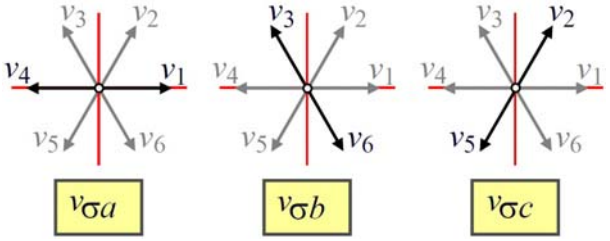

Fig. 11.- Voltage vectors applied by the inverter used to obtain the zero sequence transient voltage

$$v_{\sigma n} = \frac{(v_{an} + v_{bn} + v_{cn})}{3} \tag{14}$$

Based on this, three different zero sequence voltage vectors can be defined, $v_{\sigma a}=v_{\sigma}(1)=-v_{\sigma}(4)$; $v_{\sigma b}=v_{\sigma}(2)=-v_{\sigma}(5)$; $v_{\sigma c}=v_{\sigma}(3)=-v_{\sigma}(6)$, each obtained by applying inverter states in the *a*, *b* and *c* directions (see Fig. 11) of the complex plane. A complex voltage vector, $v_{qd\sigma}$ (15) is defined using the three measurements, which can be shown to be of the form (16), and contains information on the rotor position in its phase.

$$v_{qd\sigma} = \frac{2}{3}(v_{\sigma a} + v_{\sigma b}\, e^{j2\pi/3} + v_{\sigma c}\, e^{j4\pi/3}) \tag{15}$$

$$v_{qd\sigma} = \frac{3\Delta L_{\sigma s}\, \Sigma L_{\sigma s}\, v_{dc}}{L_{\sigma b}L_{\sigma c} + L_{\sigma a}L_{\sigma c} + L_{\sigma a}L_{\sigma b}}\, e^{jh\theta_r} = k_1\, e^{jh_r\theta_r} \tag{16}$$

Exactly the same signal processing described for the negative sequence carrier signal current (see Fig. 10), can be used for the complex voltage vector, $v_{qd\sigma}$. It is finally noted that implementation of this method requires measurement of 3 phase-to-neutral voltages (see Fig. 7c), as well as the modification of PWM patterns to obtain an adequate high frequency excitation.

VII.- Secondary saliencies decoupling and implementation issues

All the modeling and discussion presented so far has assumed that the asymmetry in the machine consisted of a single, sinusoidally varying, spatial harmonic (see (8)). This assumption is not realistic however in practice. Secondary saliencies and non-sinusoidal variation of the desired saliency always exist [11, 19-22, 24, 33] and affect to all the methods.

The secondary saliencies present in real implementations typically result in unacceptable levels of estimation error, and very often in stability concerns. Some form of compensation is therefore required. Several methods have been developed to address this issue [11, 19-22, 24, 33], most of them have the form shown in Fig. 10. An estimation of the secondary components is first measured and stored (either using time-based [24, 33] or frequency-based [17, 19, 22] look-up tables), for different operating conditions, as part of a commissioning process. The stored information is later accessed during normal sensorless operation of the drive. Artificial neural networks (ANN) have also been proposed as an alternative to the use of look-up tables for secondary saliencies decoupling [43, 44].

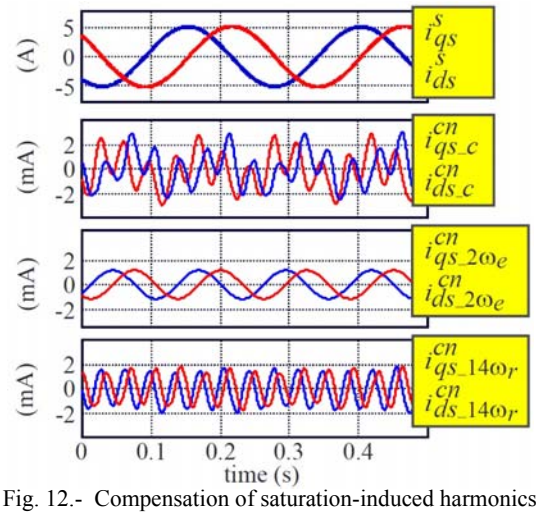

Fig. 12.- Compensation of saturation-induced harmonics

Although all the high frequency injection based sensorless control methods respond to the same physical principles, there are a number of practical implementation issues that influence the performance of each method. The non-ideal behavior of the inverter, especially inverter dead-time, has been established as one of the primary sources of error in carrier signal injection based methods. This produces a distortion in the high frequency excitation, (10), that creates additional components in the measured signals, and reduces the accuracy of the estimated position. Strategies to overcome these effects can be found in [30, 31, 41, 42].

PWM methods are less sensitive in general to effects like dead-time, since they measure the high frequency response *in the time domain*, which allows waiting until the effects due to the dead-time of the inverter have passed before making measurements. PWM methods, however, are very sensitive to parasitic effects induced in the cables and windings caused by issues like long cables, shielding of the cables, grounding strategy, etc., which can cause poorly damped, high frequency oscillations in the measured signals, strategies to mitigate these effects can be found in [32].

VIII.- Experimental results

Experimental results illustrating the performance of the sensorless methods discussed in this paper are presented in this section. Fig. 12a shows the experimentally measured stator current, while Fig 13a shows the corresponding frequency spectrum, when a high frequency voltage of the form (10) is injected in an IM. Fig. 12b shows the negative sequence carrier signal current obtained after the filtering shown in Fig. 10, while Fig. 13b shows the corresponding frequency spectrum. It is seen from Fig. 13b that the negative sequence current contains two major components: one at $(2R/p)\ \theta_r = 14\omega_r$, which is related to the rotor position (see Section II) and contains therefore the desired information, and one at $2\omega_e$, which is due to saturation, being therefore a disturbance. A look-up table was used to decouple the $2\omega_e$ component (see Fig. 10).

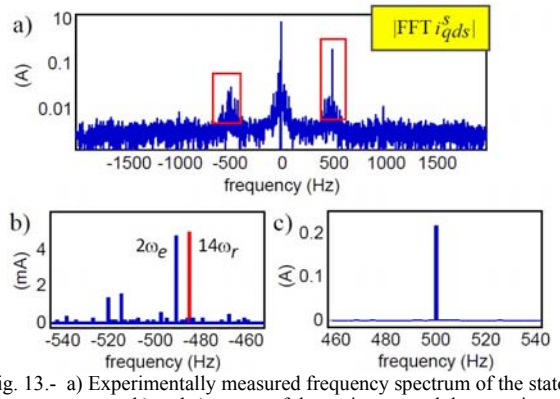

Fig. 13.- a) Experimentally measured frequency spectrum of the stator current vector, b) and c) zooms of the region around the negative and positive carrier signal current

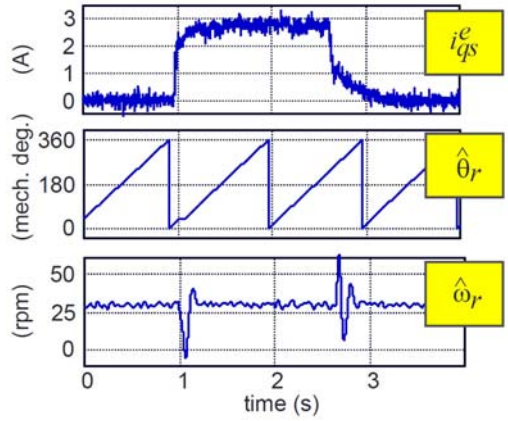

Fig. 14.- Sensorless velocity control when rated load is applied to the machine. The machine was operated at rated flux.

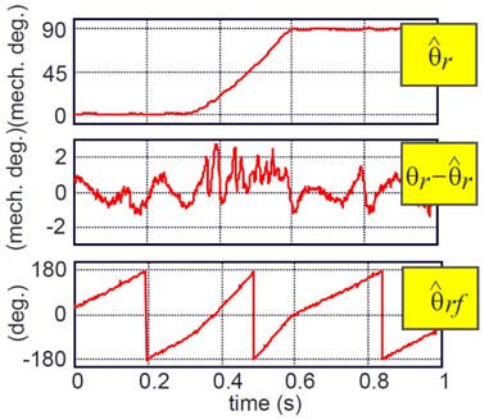

Fig. 15.- Sensorless position control when a position step from 0 to 90 degrees is commanded. The machine was operated at rated flux and 80% of rated load

Fig. 12c shows the estimated component due to saturation provided by the look-up table, while Fig. 12d shows the resulting negative sequence carrier signal current containing the rotor position information, once the saturation induced component has been decoupled. Fig 14 and 15 show examples of sensorless control using high frequency signal injection. A load-impact test is shown in Fig. 14 with the motor operation at very low speed. Sensorless position control is shown in Fig. 15. Stable, accurate control is observed in both cases.

IX.- Ongoing research

Though the basic principles of high frequency signal injection based sensorless methods were established almost two decades ago, its industrial use has been limited so far to niche applications, and cannot be considered a mature technology. There are several aspects which will need to be improved to achieve a widespread use of these techniques:

Machine design: Most of the works on high frequency signal injection sensorless control found in the literature used already existing electric machines. Secondary saliencies, mainly due to saturation produced by the fundamental current, have been repeatedly reported to be a major concern, as they affect to the salient behavior of the machine, eventually limiting the accuracy, and even compromising the stability of the sensorless control. The development of machines, mainly IPMSM, specifically designed to be used in sensorless applications, is currently an active line of research, and is expected to receive increased attention in the coming years [8-11].

Secondary saliencies decoupling: Independent of the machine design, it is practically impossible to completely avoid the presence of saturation induced saliencies. Some form of compensation is therefore needed to achieve accurate sensorless control. Many of the compensation methods reported in the literature require a laborious, time consuming, commissioning procedure. Development of new, simpler, commissioning procedures, as well as of efficient decoupling mechanisms is highly desirable [11, 19-26, 43, 44].

High frequency excitation: All the high frequency injection based sensorless methods respond to the same physical principles, what would suggest that the same performance should be obtained independent of the type of high frequency excitation being used. However, this is not true in practice, the sensitivity to implementation issues (e.g. voltage distortion due to the inverter deadtime, saturation induced saliencies, …) has been shown to depend on the high frequency excitation signal being used. Alternative forms of high frequency signal injection and signal processing are another line of research, with the goal of improving the robustness and accuracy of the sensorless control [38, 39, 45].

X.- Conclusions

Fundamental model based sensorless methods are adequate for their use in the medium-high speed range. However, they cannot operate at very low-zero speed, being unviable therefore for position control.

To overcome the limitations of fundamental model based methods, high frequency excitation sensorless control methods have been developed. This methods measure the response of the machine to some form of high frequency excitation, from which the rotor position is estimated. Several implementations of such methods have been proposed, all responding to the same physical principles, with the main differences among them being the type of high frequency signal excitation and the type and number of signals that are measured.

Active lines of research included the design of machines, mainly permanent magnet synchronous machines, suitable for their use in sensorless applications; decoupling of secondary saliencies; and alternative forms of high frequency excitation.

References

[1] Ohtani, T.; Takada, N.; and Tanaka, K., "Vector control of induction motor without shaft encoder," IEEE Trans. Ind. Appl., vol. 28, no. 1, pp. 157–165, Jan./Feb. 1992.

[2] Kubota H. and Matsuse, K., "Speed sensorless field oriented control of induction motor with rotor resistance adaptation," IEEE Trans. Ind. Appl., vol. 30, no. 5, pp. 1219–1224, Sep./Oct. 1994.

[3] Holtz, J.; , "Sensorless control of induction motor drives," *Proceedings of the IEEE* , vol.90, no.8, pp. 1359- 1394, Aug 2002.

[4] Holtz, J.; "Sensorless Control of Induction Machines—With or Without Signal Injection?," *IEEE Trans. Ind. Electr.*, vol.53, no.1, pp. 7- 30, Feb. 2006.

[5] Jansen, P.L.; Lorenz, R.D.; , "Transducerless position and velocity estimation in induction and salient AC machines," *IEEE Trans. Ind. Appl.*, vol.31, no.2, pp.240-247, Mar/Apr 1995.

[6] Robeischl, E.; Schroedl, M.; , "Optimized INFORM measurement sequence for sensorless PM synchronous motor drives with respect to minimum current distortion," *IEEE Trans. Ind. Appl.*, vol.40, no.2, pp. 591- 598, March-April 2004.

[7] Briz, F.; Degner, M.W., "Rotor Position Estimation," *Industrial Electronics Magazine, IEEE*, vol.5, no.2, pp.24,36, June 2011

[8] Bianchi, N.; Bolognani, S.;, "Influence of Rotor Geometry of an IPM Motor on Sensorless Control Feasibility," *IEEE Trans. Ind. Appl.*, vol.43, no.1, pp.87-96, Jan.-feb. 2007.

[9] Bianchi, N.; Bolognani, S.; Ji-Hoon Jang; Seung-Ki Sul; , "Advantages of Inset PM Machines for Zero-Speed Sensorless Position Detection," *IEEE Trans. Ind. Appl.*, vol.44, no.4, pp.1190-1198, July-aug. 2008.

[10] Bianchi, N.; Bolognani, S., "Sensorless-Oriented Design of PM Motors,"*Industry Applications, IEEE Transactions on*, vol.45, no.4, pp.1249,1257, July-aug. 2009

[11] Bianchi, N.; Fornasiero, E.; Bolognani, S., "Effect of Stator and Rotor Saturation on Sensorless Rotor Position Detection," *IEEE Trans. On Ind. Appl.*, vol.49, no.3, pp.1333,1342, May-June 2013

[12] Shanshan Wu; Reigosa, D.D.; Shibukawa, Y.; Leetmaa, M.A.; Lorenz, R.D.; Yongdong Li; , "Interior permanent magnet synchronous motor design for improving self-sensing performance at very low speed," *ICEMS 2008.*, pp.3278-3283, 17-20 Oct. 2008.

[13] M.W. Degner and R.D. Lorenz, "Position Estimation in Induction Machines Utilizing Rotor Bar Slot Harmonics and Carrier Frequency Signal Injection", *IEEE Trans. Ind. Appl.*, vol. 36, no. 3, May/June 2000, pp. 736 – 742

[14] Wolbank, T.M.; Metwally, M.K.; , "Sensorless control of induction machines with different designs — Impact on signal processing," *EPE '09.*, pp.1-8, Barcelona, Spain, Sept. 2009

[15] Jansen, P.L.; Lorenz, R.D.; , "Transducerless field orientation concepts employing saturation-induced saliencies in induction machines," *IEEE Trans. Ind. Appl.*, vol.32, no.6, pp.1380-1393, Nov/Dec 1996.

[16] Briz, F.; Degner, M.W.; Garcia, P.; Lorenz, R.D.; "Comparison of saliency-based sensorless control techniques for AC machines," *IEEE Trans. Ind. Appl.*, vol.40, no.4, pp. 1107- 1115, July-Aug. 2004.

[17] Garcia, P.; Briz, F.; Degner, M.W.; Diaz-Reigosa, D.; , "Accuracy, Bandwidth, and Stability Limits of Carrier-Signal-Injection-Based Sensorless Control Methods," *IEEE Trans. Ind. Appl.*, vol.43, no.4, pp.990-1000, July-aug. 2007.

[18] Raca, D.; Garcia, P.; Reigosa, D.D.; Briz, F.; Lorenz, R.D.; , "Carrier-Signal Selection for Sensorless Control of PM Synchronous Machines at Zero and Very Low Speeds," *IEEE Trans. Ind. Appl.*, vol.46, no.1, pp.167-178, Jan.-feb. 2010.

[19] Reigosa, D.D.; Garcia, P.; Raca, D.; Briz, F.; Lorenz, R.D.;, "Measurement and Adaptive Decoupling of Cross-Saturation Effects and Secondary Saliencies in Sensorless Controlled IPM Synchronous Machines," *IEEE Trans. Ind. Appl.*, vol.44, no.6, pp.1758-1767, Nov.-dec. 2008.

[20] Briz, F.; Diez, A.; Degner, M.W.; , "Dynamic operation of carrier-signal-injection-based sensorless direct field-oriented AC drives," *IEEE Trans. Ind. Appl.*, vol.36, no.5, pp.1360-1368, Sep/Oct 2000.

[21] Consoli, A.; Scarcella, G.; Testa, A.; , "Industry application of zero-speed sensorless control techniques for PM synchronous motors," *IEEE Trans. Ind. Appl.*, vol.37, no.2, pp.513-521, Mar/Apr 2001.

[22] Degner, M.W.; Lorenz, R.D.; , "Using multiple saliencies for the estimation of flux, position, and velocity in AC machines," *IEEE Trans. Ind. Appl.*, vol.34, no.5, pp.1097-1104, Sep/Oct 1998.

[23] Qiang Gao; Asher, G.; Sumner, M.; , "Sensorless Position and Speed Control of Induction Motors Using High-Frequency Injection and Without Offline Precommissioning," *IEEE Trans. Ind. Electr.*, vol.54, no.5, pp.2474-2481, Oct. 2007.

[24] Teske, N.; Asher, G.M.; Sumner, M.; Bradley, K.J.; , "Suppression of saturation saliency effects for the sensorless position control of induction motor drives under loaded conditions," *IEEE Trans. Ind. Electr.*, vol.47, no.5, pp.1142-1150, Oct 2000.

[25] Briz, F.; Degner, M.W.; Garcia, P.; Guerrero, J.M.; , "Rotor position estimation of AC machines using the zero-sequence carrier-signal voltage," *IEEE Trans. Ind. Appl.*, vol.41, no.6, pp. 1637- 1646, Nov.-Dec. 2005.

[26] Briz, F.; Degner, M.W.; Fernandez, P.G.; Diez, A.B.; , "Rotor and flux position estimation in delta-connected AC Machines using the zero-sequence carrier-signal current," *IEEE Trans. Ind. Appl.*, vol.42, no.2, pp. 495- 503, March-April 2006.

[27] Corley, M.J.; Lorenz, R.D.; , "Rotor position and velocity estimation for a salient-pole permanent magnet synchronous machine at standstill and high speeds," *IEEE Trans. Ind. Appl.*, vol.34, no.4, pp.784-789, Jul/Aug 1998.

[28] Jung-Ik Ha; Seung-Ki Sul; , "Sensorless field-orientation control of an induction machine by high-frequency signal injection," *IEEE Trans. Ind. Appl.*, vol.35, no.1, pp.45-51, Jan/Feb 1999.

[29] Jung-Ik Ha; Ide, K.; Sawa, T.; Seung-Ki Sul; , "Sensorless rotor position estimation of an interior permanent-magnet motor from initial states," *IEEE Trans. Ind. Appl.*, vol.39, no.3, pp. 761- 767, May-June 2003.

[30] Chan-Hee Choi; Jul-Ki Seok; , "Pulsating Signal Injection-Based Axis Switching Sensorless Control of Surface-Mounted Permanent-Magnet Motors for Minimal Zero-Current Clamping Effects," *IEEE Trans. Ind. Appl.*, vol.44, no.6, pp.1741-1748, Nov.-dec. 2008.

[31] Linke, M.; Kennel, R.; Holtz, J.; , "Sensorless speed and position control of synchronous machines using alternating carrier injection," *IEMDC'03*, vol.2, pp. 1211- 1217 vol.2, Madison, USA, June 2003.

[32] Holtz, J.; Hangwen Pan; , "Acquisition of rotor anisotropy signals in sensorless position control systems," *IEEE Trans. Ind. Appl.*, vol.40, no.5, pp. 1379- 1387, Sept.-Oct. 2004.

[33] Holtz, J.; Hangwen Pan; , "Elimination of saturation effects in sensorless position-controlled induction motors," *IEEE Trans. Ind. Appl.*, vol.40, no.2, pp. 623- 631, March-April 2004.

[34] Staines, C.S.; Caruana, C.; Asher, G.M.; Sumner, M.; , "Sensorless control of induction Machines at zero and low frequency using zero sequence currents," *IEEE Trans. Ind. Electr.*, vol.53, no.1, pp. 195- 206, Feb. 2006.

[35] Holtz, J.; Juliet, J.; , "Sensorless acquisition of the rotor position angle of induction motors with arbitrary stator windings," *IEEE Trans. Ind. Appl.*, vol.41, no.6, pp. 1675- 1682, Nov.-Dec. 2005.

[36] Qiang Gao; Asher, G.M.; Sumner, M.; Empringham, L.; , "Position Estimation of a Matrix-Converter-Fed AC PM Machine From Zero to High Speed Using PWM Excitation," *IEEE Trans. Ind. Electr.*, vol.56, no.6, pp.2030-2038, June 2009.

[37] C. Spiteri Staines, G. M. Asher, and K. J. Bradley, "A periodic burst injection method for deriving rotor position in saturated cage-salient induction motors without a shaft encoder," *IEEE Trans. Ind. Appl.icat.*, vol. 35, pp. 851–858, July/Aug. 1999.

[38] Hammel, W.; Kennel, R.M.; "Integration of alternating carrier injection in position sensorless control without any filtering," *ECCE 2009*, pp.3830-3836, San Jose, USA, Sept. 2009.

[39] Young-Doo Yoon; Seung-Ki Sul; Morimoto, S.; Ide, K., "High-Bandwidth Sensorless Algorithm for AC Machines Based on Square-Wave-Type Voltage Injection,"*IEEE Trans. on Ind. Appl.*, vol.47, no.3, pp.1361,1370, May-June 2011

[40] Caruana, C.; Asher, G.M.; Sumner, M.; , "Performance of HF signal injection techniques for zero-low-frequency vector control of induction Machines under sensorless conditions," *IEEE Trans. Ind. Electr.*, vol.53, no.1, pp. 225- 238, Feb. 2006.

[41] Guerrero, J.M.; Leetmaa, M.; Briz, F.; Zamarron, A.; Lorenz, R.D.; , "Inverter nonlinearity effects in high-frequency signal-injection-based sensorless control methods," *IEEE Trans. Ind. Appl.*, vol.41, no.2, pp. 618- 626, March-April 2005.

[42] Raute, R; Caruana, C; Spiteri Staines, C; Cilia, J; Sumner, M; Asher, M.; , "Analysis and Compensation of Inverter Non-linearity Effect on a Sensorless PMSM Drive at Very Low and Zero Speed Operation," *IEEE Trans. Ind. Electr.*, vol.57, no.12, pp.4065,4074, Dec. 2010.

[43] Wolbank, T.M.; Metwally, M.K.; , "Sensorless Position and Torque Control of Induction Motors Based on Transient Signal Injection and Advanced Signal Processing," *APEC 2009*, pp.216-222, Washington, USA, Feb. 2009.

[44] Garcia, P.; Briz, F.; Raca, D.; Lorenz, R. D.; , "Saliency-Tracking-Based Sensorless Control of AC Machines Using Structured Neural Networks," *IEEE Trans. Ind. Appl.*, vol.43, no.1, pp.77-86, Jan.-feb. 2007.

[45] Garcia, P.; Reigosa, D.; Briz, F.; Blanco, C.; Guerrero, J.M., "Sensorless control of surface permanent magnet synchronous machines using the high frequency resistance,"*Energy Conversion Congress and Exposition (ECCE)*, pp.2709,2716, 17-22 Sept. 2011